Available online at www.sciencedirect.com

SCIENCE DIRECT®

Catalysis Today 115 (2006) 191–198

CATALYSIS TODAY

www.elsevier.com/locate/cattod

Transient studies of carbon dioxide reforming of methane over Pt/ZrO_2 and Pt/Al_2O_3

Aisling M. O'Connor [a], Yves Schuurman [b,*], Julian R.H. Ross [a], Claude Mirodatos [b]

[a] *Centre of Environmental Research, University of Limerick, Limerick, Ireland*
[b] *Institut de Recherches sur la Catalyse, CNRS, 2 Avenue A. Einstein, 69626 Villeurbanne, France*

Abstract

The mechanism of the CO_2 reforming of methane reaction over the Pt/ZrO_2 catalyst was investigated using a temporal analysis of products (TAP) reactor system. For comparative purposes, the reaction pathway using a Pt/Al_2O_3 catalyst was also examined. A reaction sequence is suggested for both catalysts. Over both catalysts, methane decomposition takes place over platinum. The main difference between the two catalysts concerns the carbon dioxide dissociation. Over Pt/Al_2O_3 this step is assisted by hydrogen. Over Pt/ZrO_2 this step takes place over the zirconia support and involves surface vacancies. Moreover, large pools of formate and carbonate species are present on the zirconia. Transient studies conducted to determine the origin of carbon species accumulated during CO_2 reforming revealed that more than 99% of the carbon was derived from the methane molecule over both catalysts. Over the Pt/ZrO_2 catalyst, only a single very reactive carbon species was detected, while over the Pt/Al_2O_3 a second less active species was also formed.

Keywords: Temporal analysis of products; Dry reforming; Syngas; Reaction mechanism

1. Introduction

For more than a decade, the catalytic reforming of methane with carbon dioxide has stirred interest from both an environmental and an industrial perspective [1–3]. The environmental motivation stems from the fact that the reaction involves two greenhouse gases and thus could provide a means of disposing them. This is, however, not as straightforward as it seems, since this endothermic reaction requires heat input that usually is coupled to the generation of CO_2. From the industrial perspective, the reaction provides an alternative route for the production of syngas with a H_2/CO ratio near one that can be used for adjusting H_2/CO ratio in steam reforming, suitable for producing methanol or Fischer–Tropsch products. Remote natural gas reservoirs that are rich in CO_2 present another opportunity to produce economical products through this catalytic technology.

$$CH_4 + CO_2 \rightleftarrows 2CO + 2H_2 \quad (1)$$

$$CO_2 + H_2 \rightleftarrows CO + H_2O \quad (2)$$

$$2CO \rightleftarrows C + CO_2 \quad (3)$$

$$CH_4 \rightleftarrows C + 2H_2 \quad (4)$$

The main reaction (1) is accompanied by the water–gas shift reaction (2) as well as by carbon deposition through the Boudouard reaction (3) and the decomposition of methane (4). The thermodynamics for methane dry reforming predict a high potential for coke formation. Thus research is aimed at developing catalysts that do not catalyze the formation of coke.

Several studies report on the good activity and stability of Pt/ZrO_2 catalysts for the dry reforming of methane [4–16]. In order to understand the origin of the good stability of this catalyst, a temporal analysis of products (TAP) study was undertaken together with the qualitative and quantitative analysis of the coke deposits. For comparative purposes, a Pt/Al_2O_3 catalyst was also examined. TAP studies have been powerful in elucidating the reaction mechanism of dry reforming of light alkanes over a large number of different catalysts [6,17–21]. These studies show that the reaction

---

* Corresponding author. Tel.: +33 4 72 44 54 82; fax: +33 4 72 44 53 99.
E-mail address: schuurman@catalyse.cnrs.fr (Y. Schuurman).

0920-5861/$ – see front matter © 2006 Elsevier B.V. All rights reserved.
doi:10.1016/j.cattod.2006.02.051

mechanism strongly depends on both the nature of the active metal and the support.

2. Experimental

2.1. Catalyst preparation

1 wt.% Pt/ZrO_2 and 1 wt.% Pt/Al_2O_3 catalysts were prepared by wet impregnation of the calcined support with a solution of the metal salt. The ZrO_2 support was prepared by calcining $Zr(OH)_4$ extrudates supplied by Mel Chemicals XZ0706/3 in flowing air at 800 °C for 15 h. The Al_2O_3 support (Akzo Nobel α-Al_2O_3, 001-3E) was calcined using the same conditions. The calcined sample was then crushed and sieved to obtain particles in the range 212–500 μm. The support was impregnated with a solution of chloroplatinic acid (H_2PtCl_6, PGP Industries). Following equilibration overnight, the excess solvent was removed by rotary evaporation and the sample was then oven-dried at 120 °C for 2 h. The catalyst was subsequently calcined in air at 600 °C for 6 h.

The BET surface areas for the Pt/ZrO_2 and the Pt/γ-Al_2O_3 catalysts amounted to 46 and 214 m^2/g, respectively. The platinum dispersion, as determined from H_2 chemisorption, for the Pt/ZrO_2 and the Pt/γ-Al_2O_3 catalysts amounted to 49 and 62%, respectively.

2.2. TAP experiments

Transient pulse experiments were performed in a TAP-2 reactor system. In a TAP experiment, a narrow gas pulse of reactants is introduced in a microreactor that is evacuated continuously. The response of this pulse is detected by a quadrupole mass spectrometer at the reactor exit. The shape of the response reflects diffusion, adsorption, desorption and reaction, as extensively described by Gleaves et al. [22].

Two experimental formats are used in the TAP study. Multipulse experiments consist of introducing a train of pulses of one of the reactants only. These experiments will alter the surface state of the catalysts and typically will reveal information on the capacity of the catalyst to store certain species. The other experimental format is referred to as a pump–probe experiment where both reactants are admitted from two separate pulse valves. The time interval between their introductions can be varied and these experiments allow identification of the reactive surface species as well as the individual reactions step that occur. Pump–probe experiments are carried out in a cyclic fashion and thus species left on the surface during the probe pulse can interact with the reactants of the next pump pulse.

The amount of catalyst used in these experiments varied between 44 and 47 mg resulting in catalyst bed lengths of approximately 4.4 mm. Approximately, 10 mm of quartz was placed on either side of the catalyst bed to minimize the void space in the reactor. The catalyst samples were reduced in a flow of 10 $cm^3\ min^{-1}$ of H_2 for 1 h at 400 °C, after which the reactor was evacuated and heated to 600 °C at a rate of 10 °C min^{-1}. All of the TAP experiments were conducted at 600 °C.

Alternating, multipulse and simultaneous pulsing experiments were carried out using a 9:1 CH_4/Ar mixture in one valve and 9:1 $^{13}CO_2$/Ar mixture in the second valve. The number of molecules that were admitted per pulse varied between 3×10^{15} and 3×10^{16}. In the case of the alternating and simultaneous pulsing experiments, at least 20 sequences per atomic mass unit (AMU) value were monitored and averaged to improve the signal-to-noise ratio.

2.3. Transient hydrogenation experiments

A sample of 15 mg of catalyst was placed in a standard continuous flow reactor. Each sample was reduced in situ before reaction in 30 $cm^3\ min^{-1}$ of H_2. The reforming reaction was carried out at 600 °C using an isotopically labeled mixture consisting of 20% $^{13}CH_4$, 20% CO_2 and 60% He; the total flow rate used was 30 $cm^3\ min^{-1}$. Following reaction the catalyst was purged with He for 10 min. Isothermal hydrogenation was carried out at 600 °C in 30 $cm^3\ min^{-1}$of H_2 and the production of $^{13}CH_4$ and $^{12}CH_4$ was monitored using on-line MS; no products other than $^{13}CH_4$ and $^{12}CH_4$ were detected.

3. Results

3.1. $^{13}CO_2$ and CH_4 multipulse experiments over Pt/Al_2O_3 and Pt/ZrO_2

The interaction of $^{13}CO_2$ with the freshly reduced Pt/Al_2O_3 and Pt/ZrO_2 surfaces was investigated by means of $^{13}CO_2$ multipulsing over the catalysts. Fig. 1 shows the average $^{13}CO_2$ and Ar responses obtained when the first 50 pulses of $^{13}CO_2$ were passed over the catalyst at 600 °C. A broad CO_2 response curve is observed over the Pt/Al_2O_3 sample in contrast to the very narrow response curve over the Pt/ZrO_2 catalysts. The production of ^{13}CO was negligible over Pt/Al_2O_3. In the case of Pt/ZrO_2, ^{13}CO was produced even after 300 pulses of 2.4×10^{16} molecules of $^{13}CO_2$ had been admitted to the sample.

After the above experiments, in which 300 pulses of $^{13}CO_2$ were passed over both catalyst samples, multipulsing of CH_4 was carried out and the CH_4, H_2, CO and ^{13}CO responses were monitored as a function of pulse number. The areas of the peaks for each species were determined by integration and the

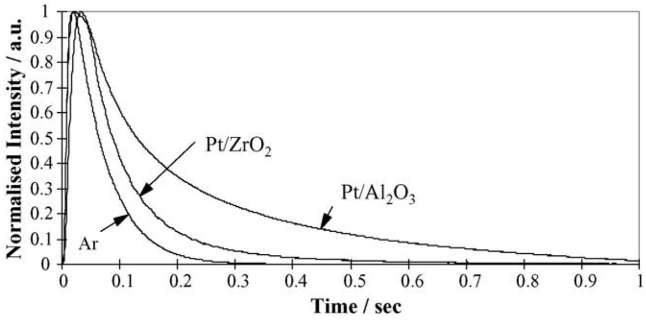

Fig. 1. The $^{13}CO_2$/Ar response on the freshly reduced Pt/ZrO_2 and Pt/Al_2O_3 catalysts; the Ar response was identical in both cases and the experiment was conducted at 600 °C.

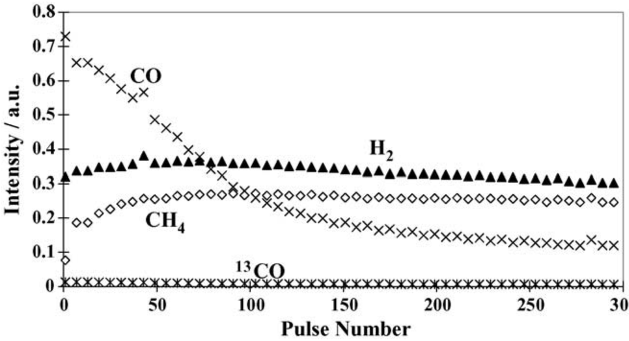

Fig. 2. CH_4 multipulse experiment after a multipulse pretreatment by $^{13}CO_2$ over the Pt/Al_2O_3 catalyst at 600 °C.

resultant intensities are shown in Figs. 2 and 3 for the Pt/Al_2O_3 and Pt/ZrO_2 materials, respectively.

In the case of the Pt/Al_2O_3 catalyst, the production of CO decreased with pulse number, reaching a constant level after approximately 175 pulses. The CO is probably formed by the reaction of surface carbon species derived from the methane molecule and surface oxygen-containing species. Based on the assumption that each molecule of CO produced required one surface oxygen atom, the surface coverage of oxygen prior to the CH_4 multipulsing experiment was calculated (i.e. after $^{13}CO_2$ multipulsing) to be 2.0 times the number of Pt atoms on the surface of the catalyst (assuming a Pt dispersion of 62%). This corresponds to approximately one hundredth of a monolayer of the entire catalyst surface (based on a BET surface area of 214 $m^2\ g^{-1}$).

Since the production of ^{13}CO was negligible during the $^{12}CH_4$ pulsing it is likely that no carbon containing species had been formed during the preceding $^{13}CO_2$ multipulsing. The methane conversion on the third pulse was 87% and it decreased slightly during the first 50 pulses, remaining constant at ca. 80% thereafter. The level of hydrogen production remained approximately constant with pulse number. The slightly higher CH_4 conversion during the first 50 pulses coincided with the production of CO; the constant levels of CH_4 consumption and H_2 production thereafter indicate that the predominant reaction is the decomposition of CH_4 and the production of H_2 and surface carbon.

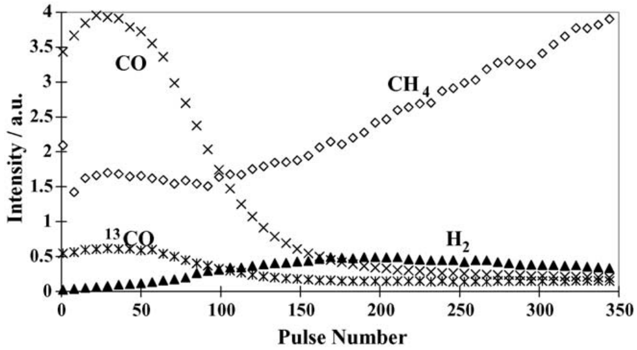

Fig. 3. CH_4 multipulse experiment after a multipulse pretreatment by $^{13}CO_2$ over the Pt/ZrO_2 catalyst at 600 °C.

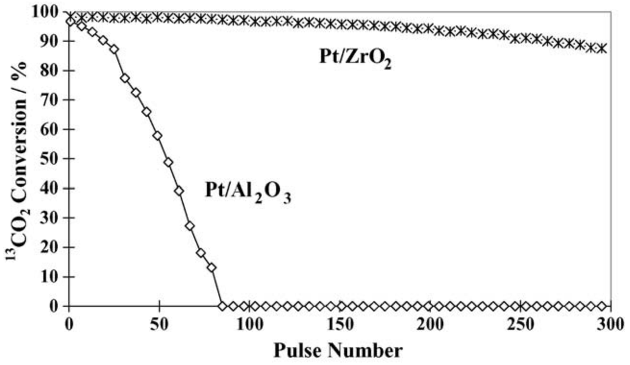

Fig. 4. $^{13}CO_2$ conversion vs. pulse number obtained during $^{13}CO_2$ multipulse experiments after multipulse CH_4 pretreatment over the Pt/Al_2O_3 and Pt/ZrO_2 catalysts at 600 °C.

Fig. 3 shows that the CO production over Pt/ZrO_2 increases during the first 25 pulses of methane and then starts to decrease quite rapidly reaching a constant level after 200 CH_4 pulses. A small but significant amount of ^{13}CO has been observed. The shapes of the ^{12}CO and ^{13}CO pulse responses were broad and very similar. The amount of oxygen present on the catalyst surface was calculated in the same way as for the Pt/Al_2O_3 catalyst; it amounted to 11.5 times the number of Pt atoms on the catalyst surface (based on a Pt dispersion of 49%) and to 20% of a monolayer coverage over the entire catalyst surface (based on a total catalyst surface area of 46 $m^2\ g^{-1}$).

The higher level of CH_4 conversion during the first 100 pulses as shown in Fig. 3 (90% of the third CH_4 pulse was consumed) is probably due to the formation of CO at this stage in the pulsing process. The CH_4 conversion began to decrease linearly after 100 pulses and on the final pulse the CH_4 conversion had decreased to 65%. The lower CH_4 conversion compared to the Pt/Al_2O_3 material indicates that the Pt/ZrO_2 catalyst does not crack CH_4 to form surface carbon as readily as does the Pt/Al_2O_3 material.

Experiments in which $^{13}CO_2$ was pulsed over both of the catalyst samples following multipulse CH_4 pretreatment were also carried out and the $^{13}CO_2$ conversions as a function of pulse number are shown in Fig. 4. Over the Pt/Al_2O_3 catalyst, 97% of the first $^{13}CO_2$ pulse was consumed and the conversion decreased rapidly with increasing pulse number, reaching zero on the 85th pulse; the conversion of subsequent pulses was negligible. In contrast, the $^{13}CO_2$ conversion over the Pt/ZrO_2 catalyst remained constant at approximately 98% during the first 100 pulses, after which it began to decrease slightly, reaching a value of 88% on the final pulse. The only product observed during these experiments over both catalysts was ^{13}CO.

3.2. Pump–probe and simultaneous pulsing experiments over Pt/Al_2O_3 and Pt/ZrO_2

A series of experiments was conducted in which methane and carbon dioxide were pulsed over the Pt/Al_2O_3 and Pt/ZrO_2 catalysts either simultaneously or with various time intervals between the reactant pulses.

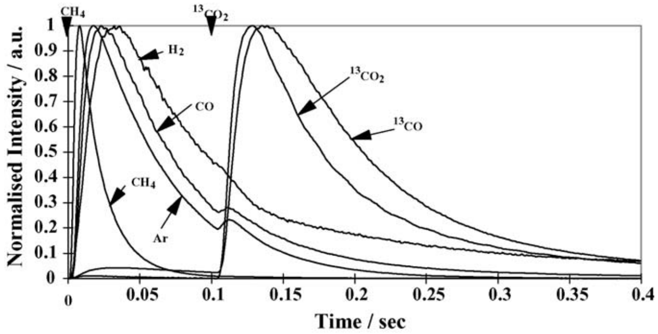

Fig. 5. Pump–probe experiment over Pt/Al_2O_3 with 0.1 s between the CH_4 and $^{13}CO_2$ pulses.

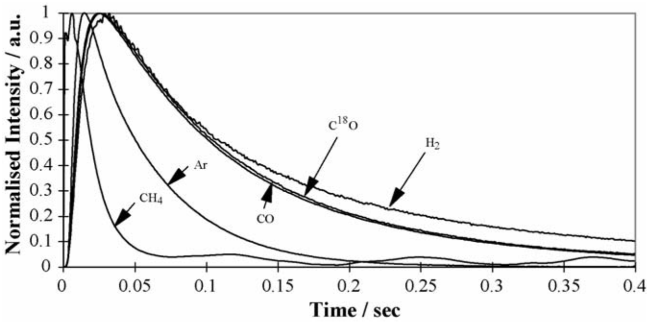

Fig. 7. The normalized responses of CH_4, Ar, CO, $C^{18}O$ and H_2 as a function of time during CH_4 pulsing in the following sequence over Pt/ZrO_2: CO_2 (200 pulses) → O_2^{18} (200 pulses) → CH_4 (200 pulses).

Figs. 5 and 6 show the average transient normalized responses of CH_4, $^{13}CO_2$, Ar, H_2, CO and ^{13}CO during pump–probe experiments in which CH_4 and $^{13}CO_2$ were pulsed alternatively every 0.1 s, over the Pt/Al_2O_3 and Pt/ZrO_2 catalysts, respectively; similar responses were obtained when the interval between the pulses were 0.2 and 0.5 s, and so these results are not shown here. In all of the pump–probe experiments conducted, CO and H_2 were formed immediately after the methane pulse and ^{13}CO was produced immediately after the $^{13}CO_2$ pulse. This indicates that dissociation of the CH_4 occurred during the methane pulse producing surface carbon species that then react rapidly with oxygen species to produce CO; when the $^{13}CO_2$ is then pulsed over the catalysts, it replenishes the surface oxygen species and ^{13}CO is produced. The CO response maximum occurred before that of H_2 over both of the catalysts. Since the pulse sizes used correspond to the pressure regime corresponding to Knudsen diffusion, the lighter H_2 would exit the reactor before CO if desorption of CO and H_2 occurred at the same rate. This, in addition to the low yields of H_2 obtained, provide evidence that there is significant interaction between H_2 and the surface of both catalysts.

The reactant conversions and product yields obtained in these experiments were calculated from the integrated non-normalized peak areas. Over the Pt/Al_2O_3, the conversion of both methane and carbon dioxide amounted to approximately 90% and they did not change by changing the interval between the two pulses. The yields of carbon monoxide were stable as well and were equal to 60 and 39% for ^{13}CO and ^{12}CO, respectively. The carbon dioxide conversion over the Pt/ZrO_2 sample was approximately 97% and stable but the methane conversion decreased from 90 to 60% when the interval between the two pulses was increased from 0.1 to 1 s. The yields of carbon monoxide were stable and amounted to 5 and 11% for ^{13}CO and ^{12}CO, respectively.

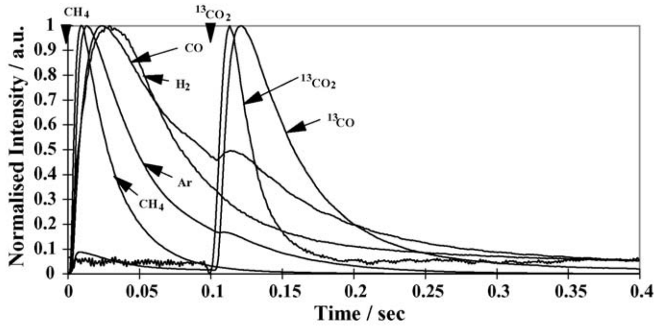

Fig. 6. Pump–probe experiment over Pt/ZrO_2 with 0.1 s between the CH_4 and $^{13}CO_2$ pulses.

The hydrogen yields were very low over both catalysts (<3.5% in all of the experiments conducted) and the water yields over both catalysts were negligible. This indicates that slow desorption of H_2 and H_2O occurred from the catalysts and indicates that storage of hydrogen-containing products occurs with both of the catalytic materials. However, the water transients are difficult to analyze and are thus omitted.

An additional experiment was carried out to ascertain the way in which the Pt/ZrO_2 catalyst stored oxygen species. The freshly reduced catalyst was first exposed to 200 pulses of CO_2 and followed by 200 pulses of $^{18}O_2$. Following this, 200 pulses of CH_4/Ar were passed over the catalyst and the CH_4, Ar, H_2, CO and $C^{18}O$ responses were monitored. The results are shown in Fig. 7. The CO and $C^{18}O$ responses were identical, indicating that these species were formed in the same step and that the oxygen species came from the same source. This indicates that the oxygen derived from the unlabeled CO_2 was stored in the same form as that from the labeled oxygen, most likely in the form of oxygen on the surface of the support.

3.3. *Transient study of carbon species formed during reaction*

In order to ascertain if CH_4 or CO_2 were completely dissociated to atomic carbon during reaction and if these species remained on the catalyst surface after reaction at 600 °C, transient isotopic experiments to examine the nature of this carbon were carried out over the Pt/ZrO_2 and Pt/Al_2O_3 catalysts. The responses to hydrogenation of the carbon species following reaction with $^{13}CH_4/CO_2$/He are shown in Fig. 8A and B for the Pt/ZrO2 and Pt/Al_2O_3 catalysts, respectively. The $^{13}CH_4$ responses observed in these figures were probably due to the hydrogenation of carbon species formed via the methane molecular route, while the much lower $^{12}CH_4$ response (≤1% of the total amount of CH_4 formed) via the carbon dioxide molecular route. Thus, it can be concluded that almost all of the

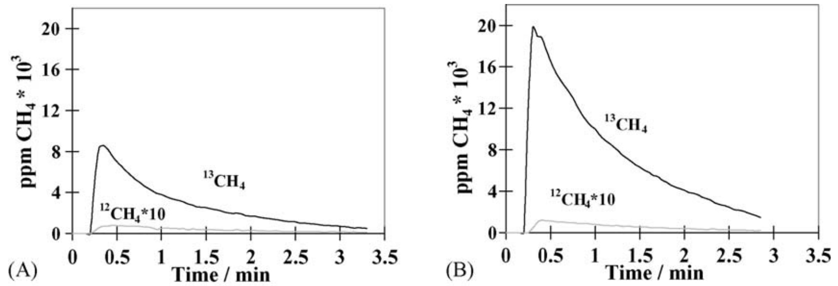

Fig. 8. Hydrogenation at 600 °C of carbon species formed after 15 min of $^{13}CH_4/CO_2$ reaction over (A) Pt/ZrO_2 and (B) Pt/Al_2O_3 (*Note*: the $^{12}CH_4$ signal is multiplied by 10 so that it can be drawn on the same scale as the $^{13}CH_4$ signal).

Table 1
Quantities of carbon deposits over Pt catalysts after dry reforming at 600 °C

	μmol C/g catalyst	
	Pt/Al_2O_3	Pt/ZrO_2
^{13}C	2500	698
^{12}C	12	7

carbon species formed on these catalysts was derived from the methane molecule. The amount of each carbon species that was formed per g of catalyst was calculated and is reported in Table 1. The amount of carbon derived from the CO_2 molecule is therefore negligible compared to the amount of carbon formed due to the decomposition of CH_4. The amount of carbonaceous species formed after 15 min of reaction over the Pt/Al_2O_3 was approximately 3.5 times the amount formed over the Pt/ZrO_2 catalyst.

Temperature programmed hydrogenation (TPH) of the carbon species formed after 15 min of CH_4/CO_2 reaction was carried out; the results obtained for the Pt/ZrO_2 and Pt/Al_2O_3 catalysts are shown in Fig. 9. Two types of residual carbon species were found on the Pt/Al_2O_3 surface after reaction: the first was a very reactive carbon species that could be hydrogenated at temperatures as low as 60 °C, while the second type of carbon required temperatures in excess of 550 °C for its removal. In contrast, only the very reactive type of carbon species was found to exist on the Pt/ZrO_2 catalyst surface after reaction.

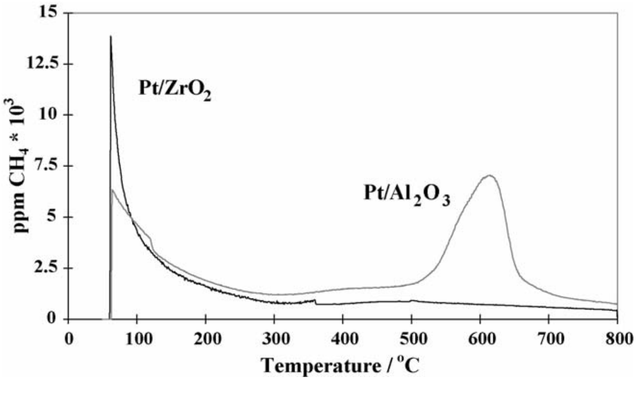

Fig. 9. Temperature programmed hydrogenation of carbon species formed after 15 min of CH_4/CO_2 reaction over Pt/Al_2O_3 and Pt/ZrO_2 catalysts.

4. General discussion

Pulsing of carbon dioxide over the two reduced samples shows directly an important difference between the two catalysts: the Pt/ZrO_2 catalyst is able to dissociate carbon dioxide in the absence of methane whereas the Pt/Al_2O_3 catalyst is not. All of the other results reported above also show a strong influence of the support on the catalytic behavior. We will present an interpretation of the results in terms of a reaction mechanism for the two samples separately, first. We will then compare the two catalysts in terms of stability.

4.1. Pt/Al_2O_3 catalyst

The freshly reduced catalyst strongly adsorbs the carbon dioxide (partly) reversibly, reflected in the strong tailing of the CO_2 response. Very little carbon dioxide dissociation occurs. Under reaction conditions the presence of carbonate and carboxylate species over Ru/Al_2O_3 has been observed by in situ DRIFTS [20]. This is a reversible interaction and does not lead to a significant CO_2 storage capacity.

The subsequent series of methane pulses confirms this by a low CO production and by the lack of ^{13}CO production. The quantity of oxygen species that reacted to form CO during CH_4 multipulsing over the Pt/Al_2O_3 catalyst (Fig. 2) corresponds to the removal of approximately two oxygen atoms per surface Pt atom. The true value will be higher, since the water formation needs to be taken into account. This quantity corresponds to only 1% of the support, but indicates a participation of alumina hydroxyl groups in the reaction scheme. A possible sequence of surface reaction steps for the formation of CO over this catalyst is the following:

Step 1: $CH_4 + 5^{*} \rightarrow C^{*} + 4H^{*}$
Step 2: $CO_2 + H^{*} \rightarrow CO^{*} + OH^{*}$
Step 3: $C^{*} + OH^{*} \rightarrow CO^{*} + H^{*}$
Step 4: $CO^{*} + OH^{*} \rightarrow CO_2{}^{*} + H^{*}$
Step 5: $OH_{al} + {}^{*} \rightarrow OH^{*} + {}_{al}$
Step 6: $OH^{*} + {}_{al} \rightarrow OH_{al} + {}^{*}$
Step 7: $H^{*} + OH^{*} \rightarrow H_2O^{*}$
Step 8: $H^{*} + H^{*} \rightarrow H_2{}^{*}$

Methane decomposition into carbon and hydrogen has been simplified, as this proceeds in several steps involving CH_x species [23]. The most abundant carbon species will probably contain some hydrogen. Reaction step 1 proceeds readily over free platinum sites as was observed during multipulse experiments. Some of this carbon probably spills over to the support as this reaction continues beyond a theoretical monolayer deposition of carbon.

Carbon dioxide dissociation over platinum is debated in the literature. van Tol et al. [24] reported that CO_2 does not dissociate over Pt, but Huinink [25] has observed oxygen exchange of CO_2. The above TAP results indicate that over a freshly reduced catalyst no significant CO_2 dissociation occurs but CO formation is observed during pump–probe experiments. A direct reaction between CO_2 and adsorbed carbon species can be excluded since very little ^{12}CO formation occurs on the $^{13}CO_2$ pulse, in contrast to what has been observed over Ni and Ru catalysts [18–21]. Apparently, no adsorbed carbon derived from the methane is left to react with the oxygen species during the carbon dioxide dissociation step, indicating that reaction steps 3 and 4 are very fast over platinum. Indeed, the pump–probe experiment (Fig. 5) shows that the pulse width of the ^{12}CO pulse derived from methane is more narrow than that of ^{13}CO on the $^{13}CO_2$ pulse, implying that carbon dioxide dissociation is the slowest step. The latter, in fact has a long tailing like the one on the $^{13}CO_2$ and a small broad pulse observed during the (next) methane pulse indicates that the carbon dioxide dissociation is still proceeding. Reaction step 2 has been proposed over Ni catalysts as well as for Rh [26–28] and seems to agree with the above results over platinum as well. Notice that hydrogen yields were very low during the TAP experiments and hydrogen is probably stored on the support in the form of hydroxyl groups through water as an intermediate. Reverse spillover can thus provide the hydrogen necessary for step 2. CO can be readily oxidized over this catalysts, thus step 4 is the reverse reaction of step 2.

Reaction steps 5 and 6 involve the spillover of hydroxyl (or adsorbed H_2O) groups from the Al_2O_3 onto the Pt and vice versa. Buyevskaya et al. [29] have reported the involvement of surface hydroxyl groups of a Rh/Al_2O_3 catalyst in the conversion of CH_x to CO under CO_2 reforming conditions. Wang and Hu drew a similar conclusion for a Rh/SiO_2 catalyst [30]. Wang et al. [31] found that water adsorbed on the Al_2O_3 support of a Rh/Al_2O_3 catalyst is a reactant in the partial oxidation of CH_4; they found that the water spilled over to the Rh where the hydroxyl groups then reacted with CH_x species to form CO. Miller et al. [32] assigned irreversible high temperature H_2 desorptions during TPD experiments over Pt/Al_2O_3 to spilt over hydrogen stabilized by the hydroxyl groups of the support. It has been reported by Peri [33] that almost complete dehydration of Al_2O_3 occurs at temperatures in excess of 800 °C; however, since this study was conducted at 600 °C it is likely that desorption of water does not occur to a large extent and that the surface OH species are sufficiently mobile for spillover to occur from the support onto the Pt.

4.2. Pt/ZrO_2 catalyst

Carbon dioxide reacts readily over the freshly reduced catalyst with the formation of ^{13}CO. The Pt/ZrO_2 catalyst is thus able to retain oxygen abstracted from the carbon dioxide. Carbon dioxide and carbon monoxide are also adsorbed irreversibly, as there was a large deficiency in the carbon mass balance. The formation of ^{13}CO on the methane pulse directly after the train of carbon dioxide pulses (Fig. 3) confirms the existence of a pool of carbonates on Pt/ZrO_2.

By using in situ FTIR spectroscopy, Kalies et al. [34] have shown that carbon monoxide adsorbs on ZrO_2 and on Pt/ZrO_2 at 638 K and leads to the formation of formate and carbonate species. Moreover, carbonate species were detected by DRIFTS when CO_2 was passed over the Pt/ZrO_2 catalyst as well as over the zirconia support [35].

From the multipulse of methane experiment, it has been calculated that the O/Pt ratio amounts to 11 corresponding to 20% of support monolayer. Again, the actual value will be higher, since the water formation has not been taken into account. In addition, the participation of oxygen of the zirconia using a Rh/ZrO_2 catalyst was reported by Efstathiou et al. [36] and van Keulen et al. [6] reported the existence of an oxygen pool during CO_2 reforming over a Pt/ZrO_2 catalyst. The ratio of ^{12}CO to ^{13}CO during this methane multipulse experiment is approximately 7, thus apparently oxygen species to oxidize the carbon are more readily available than carbonate species.

The following reaction steps over Pt/ZrO_2 can thus be proposed:

Step 1: $CH_4 + 5^{*} \rightarrow C^{*} + 4H^{*}$
Step 2: $CO_2 + \square_{Zr} \rightarrow CO^{*} + O_{Zr}$
Step 3: $CO|_{Zr} + OH_{Zr} \rightarrow HCOO|_{Zr}$
Step 4: $CO_2|_{Zr} + OH_{Zr} \rightarrow HCO_3|_{Zr}$
Step 5: $HCO_3|_{Zr} + \square_{Zr} + {}^{*} \rightarrow CO_{*} + OH_{Zr} + O_{Zr}$
Step 6: $C^{*} + O_{Zr} \rightarrow CO^{*} + \square_{Zr}$
Step 7: $H^{*} + O_{Zr} \rightarrow OH^{*} + \square_{Zr}$
Step 8: $H^{*} + OH^{*} \rightarrow H_2O^{*}$
Step 9: $H^{*} + H^{*} \rightarrow H_2^{*}$

The same step for methane decomposition is proposed for the Pt/ZrO_2 catalysts as for the Pt/Al_2O_3 catalyst. However, the methane multipulse experiments indicate that this decomposition seems to proceed slower over the Pt/ZrO_2 sample once most of the available oxygen has been consumed than over Pt/Al_2O_3. Nagaoka et al. [14] reached a similar conclusion from their TPO and TPRn experiments. No significant spillover of carbon to the zirconia seems to occur.

Carbon dioxide dissociation proceeds completely differently over Pt/ZrO_2 and involves a zirconia site, based on the arguments given above. In step 2, $\square_{Zr}$ is an oxygen vacancy at the zirconia surface and O_{Zr} is an oxygen surface species. It is most likely that these species are located at the Pt/zirconia interface, as Bitter et al. [7] have shown that the activity can be correlated to the available $Pt–ZrO_2$ perimeter. As mentioned above, Efstathiou et al. [36] suggested the participation of zirconia lattice oxygen and lattice vacancies. The TAP results suggest that these species are restricted to the surface only. These oxygen surface species can be replenished either by CO_2 or by O_2, as has been demonstrated by pretreating the catalyst by a CO_2, $^{18}O_2$ mixture.

The carbon derived from the methane reacts with the surface oxygen species that are at the Pt–ZrO_2 interface (step 6). Oxidation of hydrogen occurs in an analogous way.

Steps 3 and 4 represent the adsorption and storage of CO and CO_2 on the zirconia support. A two-step mechanism involving direct CO adsorption on zirconia followed by step 3 has been reported for the formation of formate species [37]. The carbonate species can decompose into CO and O_{Zr}, when Zr vacancies are available (step 5). During the $^{13}CO_2$ multipulse experiment both carbon dioxide decomposition and $^{13}CO_2$ storage take place, which will sature the Zr vacancies. Then, during the methane multipulse experiment methane is oxidized into CO and this leads to new Zr vacancies that will allow the decomposition of the stored labeled carbonate species into O_{Zr} and ^{13}CO. The reaction steps proposed above are in agreement with the reaction mechanism based on in situ DRIFTS studies first proposed in ref. [35] and confirmed by the work of Lercher and co-workers [7,9,12].

4.3. Carbon formation

In the present study, more than 99% of the carbonaceous species originated from the CH_4 molecule. The decomposition of CH_4 is therefore the primary reaction leading to the formation of surface carbon species over the Pt/Al_2O_3 and Pt/ZrO_2 catalysts. This is in agreement with the study by Nagaoka et al. [14].

The hydrogenation of the coke deposits after dry reforming at 600 °C shows that a much larger quantity of coke is formed over Pt/Al_2O_3 than over Pt/ZrO_2. The TPH experiment shows that this extra amount of carbon species present on the Pt/Al_2O_3 are essentially coke deposits that are hydrogenated at high temperatures. Bitter et al. [12] also found a much higher rate of carbon formation on Pt supported on Al_2O_3 or TiO_2 compared to Pt/ZrO_2 during CO_2 reforming. Zhang et al. [38] have also observed that higher amounts of carbon were formed on a Rh/Al_2O_3 catalyst compared to those on Rh/ZrO_2; after 2 h on stream 0.26 equivalent monolayers of carbon per Rh atom had formed compared on the Rh/Al_2O_3 catalyst to 0.03 in the case of the Rh/ZrO_2 material. Nagaoka et al. [14] observed two TPO peaks after dry methane reforming over a Pt/Al_2O_3 catalyst. They attributed the lower temperature peak to coke on the platinum and the high temperature peak to coke deposited on the alumina support. For the Pt/ZrO_2, they observed only coke deposition on the Pt and not on the zirconia, which they attributed to the lower concentration of Lewis acids sites on the zirconia than on the alumina.

Since the Pt/Al_2O_3 catalyst deactivates during the CO_2 reforming of methane and the Pt/ZrO_2 catalyst remains stable, the formation of the high temperature, less reactive carbon might be the cause of this deactivation.

5. Conclusions

Over both catalysts methane decomposition takes place over platinum. The main difference between the two catalysts concerns the carbon dioxide dissociation. Over Pt/Al_2O_3 this step is assisted by hydrogen. Over Pt/ZrO_2, this step takes place over the zirconia support and involves surface vacancies. Moreover, large pools of formate and carbonate species are present on the zirconia. Both the Pt/ZrO_2 and Pt/Al_2O_3 have large storage capacities for hydrogen that is probably retained on the catalyst support in the form of hydroxyl groups.

Further transient experiments revealed that the carbonaceous species that had accumulated on the catalyst surface during reaction were mostly derived from the CH_4 molecule, the CO_2 contributing to less than 1% of the total amount of carbon. Over the Pt/ZrO_2 catalyst all of the carbon formed was very active towards hydrogenation and was therefore probably a reaction intermediate; however, a second less active carbon species was also formed over the Pt/Al_2O_3 catalyst and this species was thought to lead to the deactivation of the catalyst.

References

[1] J.R. Rostrup-Nielsen, Catal. Today 18 (1993) 305.
[2] S. Teuner, Hydrocarb. Process. (1985) 106.
[3] A.M. Gadalla, B. Bower, Chem. Eng. Sci. 43 (1988) 3049.
[4] J.H. Bitter, W. Hally, K. Seshan, J.G. van Ommen, J.A. Lercher, Catal. Today 29 (1996) 349.
[5] A.N.J. van Keulen, M.E.S. Hegarty, J.R.H. Ross, P.F. van den Oosterkamp, Stud. Surf. Sci. Catal. 107 (1997) 537.
[6] A.N.J. van Keulen, K. Seshan, J.H.B.J. Hoebink, J.R.H. Ross, J. Catal. 166 (1997) 306.
[7] J.H. Bitter, K. Seshan, J.A. Lercher, J. Catal. 171 (1997) 279.
[8] M.C.J. Bradford, M.A. Vannice, J. Catal. 173 (1998) 157.
[9] J.H. Bitter, K. Seshan, J.A. Lercher, J. Catal. 176 (1998) 93.
[10] M.E.S. Hegarty, A.M. O'Connor, J.R.H. Ross, Catal. Today 42 (1998) 225.
[11] A.M. O'Connor, J.R.H. Ross, Catal. Today 46 (1998) 203.
[12] J.H. Bitter, K. Seshan, J.A. Lercher, J. Catal. 183 (1999) 336.
[13] S.M. Stagg-Williams, F.B. Noronha, G. Fendley, D.E. Resasco, J. Catal. 194 (2000) 240.
[14] K. Nagaoka, K. Seshan, K. Aika, J.A. Lercher, J. Catal. 197 (2001) 34.
[15] M.M.V.M. Souza, D.A.G. Aranda, M. Schmal, J. Catal. 204 (2001) 498.
[16] F.B. Noronha, E.C. Fendley, R.R. Soares, W.E. Alvarez, D.E. Resasco, Chem. Eng. J. 82 (2001) 21.
[17] Y. Schuurman, V.C.H. Kroll, P. Ferreira-Aparicio, C. Mirodatos, Catal. Today 38 (1997) 129.
[18] A. Slagtern, Y. Schuurman, C. Leclercq, X. Verykios, C. Mirodatos, J. Catal. 172 (1997) 118.
[19] Y. Schuurman, C. Marquez-Alvarez, V.C.H. Kroll, C. Mirodatos, Catal. Today 46 (1998) 207–214.
[20] P. Ferreira-Aparicio, C. Marquez-Alvarez, I. Rodriguez-Ramos, Y. Schuurman, A. Guerrero-Ruiz, C. Mirodatos, J. Catal. 184 (1999) 202–212.
[21] A. Olafsen, Å. Slagtern, I.M. Dahl, U. Olsbye, Y. Schuurman, C. Mirodatos, J. Catal. 229 (1) (2005) 163.
[22] J.T. Gleaves, G.S. Yablonskii, P. Phanawadee, Y. Schuurman, Appl. Catal. A: Gen. 160 (1997) 305.
[23] A.D.E. Koster, R.A. van Santen, J. Catal. 127 (1991) 141.
[24] M.F.H. van Tol, A. Gielbert, B.E. Nieuwenhuys, Appl. Surf. Sci. 67 (1993) 166.
[25] J.P. Huinink, Doctorate Thesis, Eindhoven University of Technology, The Netherlands, 1995.
[26] M.C. Bradford, M.A. Vannice, Appl. Catal. 142 (1996) 73.
[27] M.C. Bradford, M.A. Vannice, Appl. Catal. 142 (1996) 97.
[28] A. Erdöhelyi, J. Cserényi, F. Solymosi, J. Catal. 141 (1993) 287.
[29] O.V. Buyevskaya, D. Wolf, M. Baerns, Catal. Lett. 29 (1994) 249.
[30] H.Y. Wang, C.T. Hu, Appl. Catal. A: Gen. 155 (1997) 239.

[31] D. Wang, O. Dewaele, A.M. De Groote, G.F. Froment, J. Catal. 159 (1996) 418.

[32] J.T. Miller, B.L. Meyers, F.S. Modica, G.S. Lane, M. Vaarkamp, D.C. Koningsberger, J. Catal. 143 (1993) 395.

[33] J.B. Peri, J. Phys. Chem. 69 (1965) 211.

[34] H. Kalies, N. Pinto, G.M. Pajonk, D. Bianchi, Appl. Catal. A: Gen. 202 (2000) 197.

[35] A.M. O'Connor, F.C. Meunier, J.R.H. Ross, In: A. Parmaliana et al. (Eds.), Stud. Surf. Sci. Catal., vol. 119, 1998, p. 819.

[36] A.M. Efstathiou, A. Kladi, V.A. Tsipouriari, X.E. Verykios, J. Catal. 158 (1996) 64.

[37] X. Mugnery, T. Chafik, M. Primet, D. Bianchi, Catal. Today 52 (1999) 15.

[38] Z.L. Zhang, V.A. Tsipouriari, A.M. Efstathiou, X.E. Verykios, J. Catal. 158 (1996) 51.